

Discontinuity of diurnal temperature range along elevated regions

Yi-Shin Jang^{1*}, Sheng-Feng Shen², Jehn-Yih Juang³, Cho-ying Huang³, Min-Hui Lo¹

¹Department of Atmospheric Sciences, National Taiwan University, Taipei, Taiwan

²Biodiversity Research Center, Academia Sinica, Taipei, Taiwan

³Department of Geography, National Taiwan University, Taipei, Taiwan

*Corresponding author: Yi-Shin Jang (D08229003@ntu.edu.tw)

Key Points:

- A relatively great variance of daily temperature range between the open fields and understory at high altitudes.
- Canopy shade efficiently moderates the diurnal variability and the elevational variation of daily temperature range.
- The fog and low-clouds create altitudinal discontinuities in daily temperature range.

Abstract

Low-clouds and fog moderate the diurnal temperature range (DTR) through radiative effects. Consequently, frequent foggy events make montane cloud forests (MCFs) stable and unique. However, observations in the understory of the forest are rare. To investigate the DTR variation in elevations, we surveyed the Central Cross-Island Highway in central Taiwan transects with MCFs. The results from paired weather stations revealed that the DTR increases significantly with altitude in open fields but not in the forest's understory. Furthermore, the continuous observations in altitude across non-cloud forest and MCFs indicate that DTR decreases in both the open field and understory of MCFs. The DTR discontinuity highlights the indispensability of MCF for the mountain ecosystem. Further simulating the integrative effect of the climate and land-use change on fog is crucial for the ecoclimate in mountainous regions.

Plain Language Summary

The diurnal temperature range (DTR), regulated by canopy and fog, is critical to the ecosystem. During the day, fog and the canopy block downward solar radiation to prevent the increase in temperature. At night, fog and the canopy trap long-wave radiation to reduce the rate of temperature decline. Observational data indicate that DTR increases significantly with altitude in open fields but not in the understory. Therefore, the difference in DTR between open fields and the understory is more significant at a higher altitude. Furthermore, the difference in the DTR is lower at midaltitude, which is most likely related to the presence of montane cloud forests. DTR discontinuity at high altitudes highlights the value of montane cloud forests.

1 Introduction

Mountains provide essential, diverse habitats and elevational gradients that critically enable species to respond to the crisis of migration or extinction. Previous studies have explored the effect of increasing average temperature on the survival and distribution of organisms (Chen et al., 2009; Kerr et al., 2015; Rumpf et al., 2018). In fact, in addition to temperature, other environmental variations cause critical stress to living organisms. The diurnal temperature range (DTR), which is a relatively short temporal variation, can greatly influence species distribution (W.-P. Chan et al., 2016). The DTR is defined as the range enclosed by the daily maximum and minimum temperatures (T_{\max} and T_{\min} , respectively), and a key indicator that provides more information than the mean temperature in determining the effect of climate change (Braganza et al., 2004; Easterling et al., 1997). Forests cover about a quarter of the global mountain area and is the most diverse terrestrial system, but in the meantime, the most threatened ecosystem worldwide (Körner, 2004). Biotic and abiotic features, for example, the canopy and topography, create a unique microclimate and exert moderating effects that encourage species abundance (De Frenne et al., 2013; Zellweger et al., 2019). Particularly, the disparate shade and canopy modulation intercepting the downward radiation cause thermal variations in space (Klinges & Scheffers, 2021). However, traditional weather stations are located on flat terrain with uniform grass, and observational data from mountainous regions are rare (Nicolas Pepin et al., 2015; Nick Pepin et al., 2019). Even though the contrast between open field and understory had been mentioned in the previous study, two stations were located more than 100 km away with various synoptic environmental conditions (Rapp & Silman, 2012). Therefore, high-resolution in-situ observations in the understory and open fields within a reasonably close distance in mountainous regions are crucial for studying the critical role of forest in the micro-eco-climatological systems.

Most previous studies have focused on how the DTR varies over time (Easterling et al., 1997; Jaagus et al., 2014; Kumar et al., 1994; Nick Pepin et al., 2019; Shekhar et al., 2018; Shen et al., 2014; Vose et al., 2005; Zhang et al., 2021). Comparatively, the trends of DTR in altitude were not consistent both in the open field (Gheyret et al., 2020; Rapp & Silman, 2012) and understory (Rapp & Silman, 2012; Wang et al., 2017; Xue et al., 2020). The occurrence of dynamic clouds, fog, and rainfall might have a narrow DTR (Dai et al., 1999; Hansen et al., 1995; Jackson & Forster, 2010; Karl et al., 1993; Rapp & Silman, 2012) and cause the uncertainty of elevational trends in DTR. Nevertheless, those studies usually focused on either single-point in-situ observations or regional data with a coarse resolution. Thus, to understand the altitudinal gradient of the DTR along the continuous mountain range, a comparison of low-clouds and fog in montane cloud forests (MCFs) is necessary (Myers et al., 2000). Additionally, the steep terrain, surrounding ocean, and prevailing seasonal winds make Taiwan have the highest percentage of cloud forest in the world (Bruijnzeel et al., 2011; Schulz et al., 2017). Thus, this study used in-situ paired weather station observations in open fields and the understory to explore how the canopy shade influences the altitudinal gradient of diurnal variation across non-cloud forests and MCFs in Taiwan.

2 Data and Methods

2.1 Study sites

The study region was selected over the east-facing slope of the Central Cross-Island Highway (CCH) from 100 to 3250 m a.s.l. (Fig. 1a) in 2018–2019. The 15 study sites were along the CCH with an elevation interval of approximately 250 m (Fig. 1b). Eleven paired meteorological stations were installed on opposite sides of the road to demonstrate the microclimate contrasts between the understory and open fields. The paired stations are as close as possible (10–500 m apart) in order to eliminate the effect of synoptic weather conditions and landscapes. Four additional unpaired meteorological stations were also installed along the study transect to increase the spatial resolution. All sites were placed around 1–2 m away from the road to constrain the edge effect.

The transect crosses the non-cloud forest and the MCFs. The characteristic features of MCFs in Taiwan are distributed from 1500 to 2000 m a.s.l., whereas in some monsoon-affected areas, the MCFs might extend down to 1000 m a.s.l. (Schulz et al., 2017). Therefore, based on the MCF map stated by Schulz et al. (2017), we extracted four study sites, located in the MCFs region from 1250 to 2000 m a.s.l. (Fig. 1b), to represent the microclimate of MCFs in the mid-elevational region in CCH. Furthermore, before conducting the formal integrated observation, we carried out observation over an intensive observing period (IOP) to explore the effect of fog on the east-facing slope of the CCH. The study site of IOP was located in the open fields at 1500 m a.s.l. from 2017/04/25–2017/06/07. In addition to air temperature, the relative humidity (RH) and visibility data were recorded during the IOP.

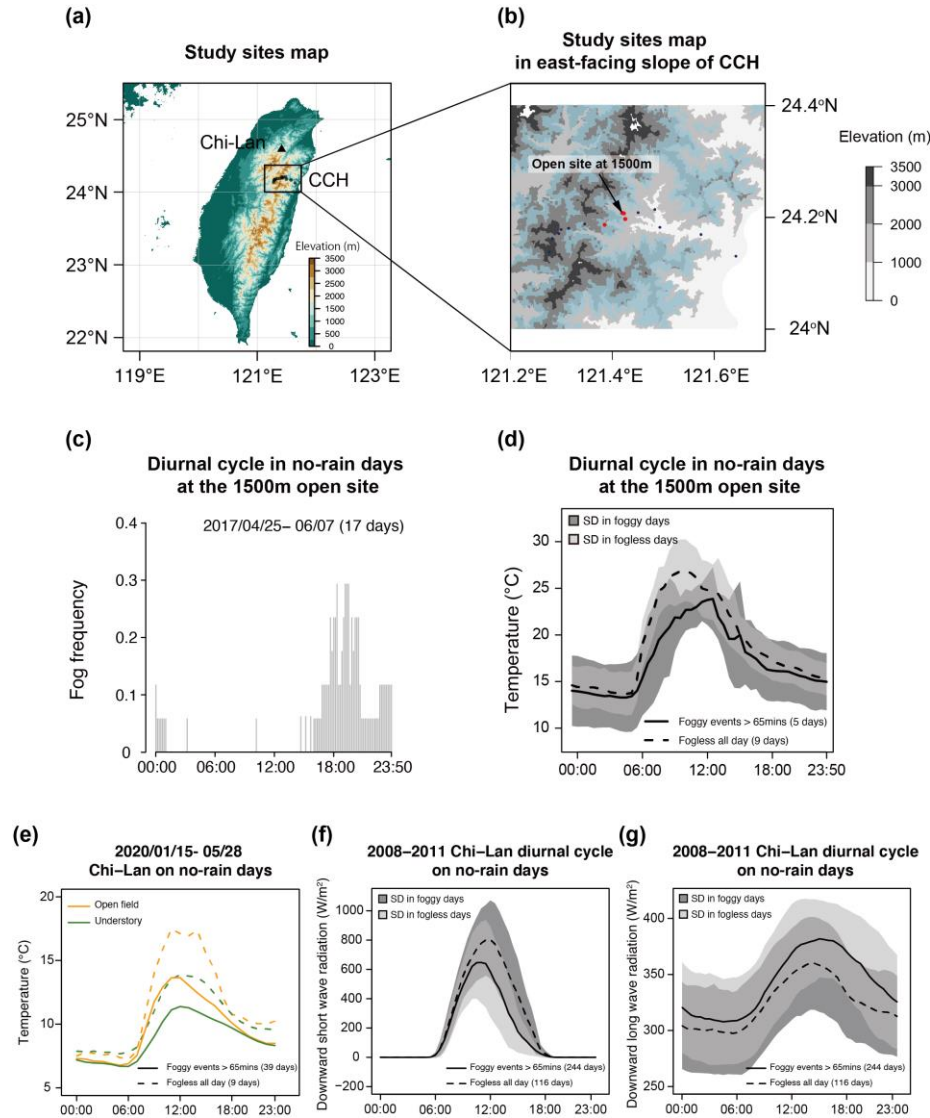


Figure 1. (a) Locations of Chi-Lan and the Central Cross-Island Highway (CCH) in Taiwan. (b) A closer look of CCH with sites along an elevation gradient. The light blue area is the MCF by Schulz et al. (2017). (c) The diurnal cycle of fog frequency at CCH 1500 m a.s.l. in IOP. The gray bars represent the probability of fog occurrence for each hour. (d) The diurnal cycle air temperature during IOP (e–g) Diurnal cycles on no-rain days in Chi-Lan during 2020/01/15–05/28 and 2008 to 2011. The orange line represents the mean observational air temperature every hour in the open field, and the green line represents the understory. Solid lines represent the mean of the observational data every half hour in the foggy days as fog events span > 65 minutes. Dashed lines represent the fogless days. The grey shaded areas represent the mean \pm 1 standard deviation.

To understand the distinctive features of MCFs, we also selected Chi-Lan, a typical MCF in northeastern Taiwan (Fig. 1a). In Chi-Lan, frequent fog events occurred approximately 33% of the time during 2008–2011 (Gu et al., 2021). To compare the effect of fog on the DTR in open fields and the understory, we paired sites in Chi-Lan within 300 m

horizontally. The paired meteorological stations in Chi-Lan were installed at 1.5 m above the ground in the understory of forest (1650 m a.s.l., 24°35'N, 121°25'E) and on a flat grassland without tree canopy (canopy, hereafter) cover (1711 m a.s.l., 24°35'N, 121°24'E), respectively.

2.2 Meteorological Data

In the CCH, we acquired air temperature and RH by using a HOBO microstation data logger (U21-002; Onset, Cape Cod, MA, USA) with a 12-bit Temperature Smart sensor (S-THB-M002) and iButton® devices (Maxim Integrated Products, Sunnyvale, CA, USA). The iButton® device is an autonomous system with a data logger and temperature sensor that measures temperature and records the data in a 512 bytes memory section. A polyvinyl chloride shield was used to prevent exposure to solar radiation (S. Chan et al., 2019; Tsai et al., 2020). The data logger was nailed to a tree trunk 120–150 cm above the ground in the open field. Air temperature was recorded every 30 minutes by using iButton® devices and every 10 minutes by using the HOBO microstation data logger. After averaging raw data to hourly data, the data quality was checked by removing the spikes beyond the triple standard deviation of each hour. The daily DTR was derived from the difference between daily maximum and minimum temperature. We note that only the data with missing value less than 4 hours in one day were obtained. In IOP, visibility was measured with a MiniOFS sensor (Sten Löfving, Optical Sensors, Göteborg, Sweden) every 10 min at 1500 m a.s.l. in the open site. We adopted the World Meteorological Organization's definition of a foggy event as one where visibility < 1000 m. The definition of foggy days without rain during IOP in CCH was the total occurrence of fog events more than 65 minutes, the third quantile of the daily duration of foggy condition.

In Chi-Lan, air temperature in the understory were obtained from the weather station (EM50, METER Group, Pullman, WA, USA), which comprised a humidity and temperature sensor (ATMOS 14, METER Group). We use the Yuanyanghu weather station (C0UA1) of Central Weather Bureau in Taiwan, which was located 300 m away from the understory site. In addition, solar radiation, longwave radiation, and visibility (Mira 3544, Aanderaa Data Inst., Bergen, Norway) measurements were obtained from the top of the Chi-Lan flux tower (Chu et al., 2014).

2.3 Leaf Area Index

In addition to the dynamic variations in clouds and fog, the complicated topographic shade and diverse dense canopy might exert a complex influence on the spatial variation in the DTR. The canopy efficiently prevents heating caused by solar radiation, reducing the T_{\max} during the day (Scheffers et al., 2014; Zellweger et al., 2019). Thus, to evaluate the effect of canopy cover on the DTR, we applied the leaf area index (LAI), defined as the one-sided green leaf area per unit ground surface area, to represent the canopy cover density at every site. The LAI data were extracted from the LAI product (MCD15A3H) of the Moderate Resolution Imaging Spectroradiometer (MODIS) for 2018–2019 by using the R package MODIS tools (Hufkens et al., 2018).

2.4 Aspect

Due to the probability of higher daytime temperature at the east-facing side, the effect of aspect on daytime temperature should also be considered. We used the following formula for transforming the aspect along the north to south-facing slope in the linear regression analysis (Beers et al., 1966):

$$A_t = \cos (A_{\max} - A) \quad (1)$$

After transforming, A_t represents effective exposure to the solar radiation, rescaled to from -1 to 1. The maximum exposure to solar radiation, A_{\max} , is 90° for the east-facing side. A is the original aspect, computed from a 20 m gridded digital elevation model provided by the Ministry of the Interior in Taiwan (https://www.tgos.tw/TGOS/Web/MetaData/TGOS_Query_MetaData.aspx?key=TW-06-301000000A-612640). We computed the aspect of each site by using the R package raster (Hijmans et al., 2015) with eight neighboring grids.

2.5 Data Analysis

We took that information apart from the effect of elevation by following steps to emphasize the unique features in the mid-elevational regions. First, we interpolated the DTR in the midpoint of each elevational region by the linear regression of DTR and elevation, as the predicted DTR. The detrended DTR were obtained by subtraction the actual DTR from the predicted DTR in every elevational region to conclude the effect of fog and cloud without accounting for the elevational impact. We compared the difference of detrended DTR between mid-elevation and other elevated to determine whether the elevational trend of DTR is influenced by fog and low-clouds.

To examine the different trends in altitude of T_{\max} and T_{\min} , we performed an analysis of covariance (ANCOVA) using the R function `anova_test()` function from the package "rstatix" of R (Kassambara, 2020). In the analysis, a multiple regression was created with an interaction term between T_{\max} or T_{\min} and elevation to examine the homogeneity of regression slopes. The significance of the coefficient of the interaction term represent whether the slope among the elevational trends of T_{\max} and T_{\min} is heterogeneous.

3 Results

From the observed results on no-rain days during IOP, the probability of a foggy event lasting more than one hour is approximately 30% (Fig. 1c), and the DTR was smaller during the foggy days at 1500 m in CCH (Fig. 1d). Consequently, we applied observational data from Chi-Lan using the same definition of foggy days in CCH to determine how the foggy events influence the diurnal radiation. In Chi-Lan, the DTR was narrower during foggy days both in the open field and understory sites during the observational period of 2011 (Fig. 1e). During foggy days, low solar radiation penetration (Fig. 1f) limited the increase in daytime temperature, and downward longwave radiation (Fig. 1g) caused an increased nighttime temperature. Fog might efficiently narrow the DTR of MCFs, resulting in a unique and stable elevational region in the mountain forest ecosystem.

3.1 Canopy Shade Moderates Spatial Variance in the Understory

To comprehend the difference in microclimates between the traditional meteorological observation and realistic habitat, we compared the observations of the open field and understory. We found that the DTR was positively correlated with the elevation in open sites (slope = $1.25^{\circ}\text{C}/\text{km}$, $R^2 = 0.48$, $p < 0.002$; Fig. 3a). Nevertheless, no significant elevational trends of the DTR were observed in the understory. The elevational trends of the DTR were determined based on variation in the T_{max} and T_{min} in altitude. In the open field, the T_{min} ($T_{\text{min}}^{\text{open}}$, hereafter) declined more substantially than the T_{max} ($T_{\text{max}}^{\text{open}}$, hereafter) in altitudes ($p < 0.02$), which contributed to an increase in the DTR ($T_{\text{max}}^{\text{open}}$: slope = $-3.61^{\circ}\text{C}/\text{km}$, $R^2 = 0.87$, $p < 0.001$; $T_{\text{min}}^{\text{open}}$: slope = $-4.85^{\circ}\text{C}/\text{km}$, $R^2 = 0.99$, $p < 0.001$; Fig. 2b). In the understory, the decreasing rate of the T_{max} ($T_{\text{max}}^{\text{under}}$: slope = $-4.81^{\circ}\text{C}/\text{km}$, $R^2 = 0.97$, $p < 0.001$) and T_{min} ($T_{\text{min}}^{\text{under}}$: slope = $-5.07^{\circ}\text{C}/\text{km}$, $R^2 = 0.99$, $p < 0.001$; Fig. 2c) at elevated regions were similar ($p = 0.301$), resulting in insignificant trend ($R^2 = 0.08$, $p = 0.30$) of the DTR at elevated regions.

2018–2019 East-facing slope of CCH in Taiwan

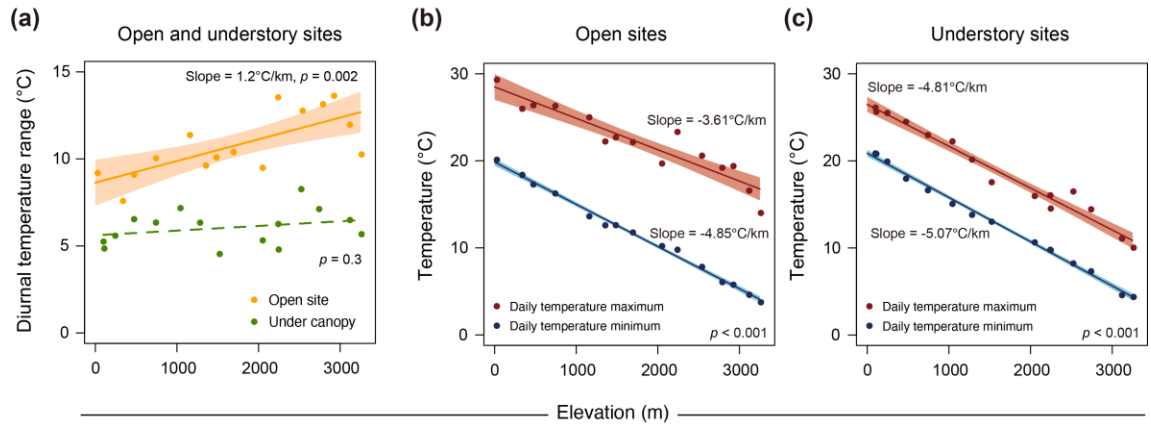


Figure 2. (a) Elevational pattern of DTR from 2018 to 2019. Solid circles are the averaged DTR of every observational site in the understory and open field. The elevational pattern of T_{max} and T_{min} from 2018 to 2019 in the (b) open field and (c) understory. Solid circles are the averaged T_{min} and T_{max} of every observational site in the understory and open fields. Lines represent the least-squared means, and shaded areas represent 95% confidence intervals. The dashed line indicates no significance.

3.2 Discontinuous Trend of DTR at High Altitudes

In addition to indicating the effect of the forest on the elevational variation of the DTR, our result further suggested a discontinuous feature of the DTR along the elevation in both the open field and understory (Fig. 2a). We compared the difference in the DTR between MCF and other elevational regions to investigate the unique characteristics of MCFs. After eliminating the elevational trend, whether in the open field or understory, the DTR in MCFs was significantly smaller than that at low and high elevations (Fig. 3a,

b). The discontinuous changes of DTR in altitude or the elevational trend of DTR changes drastically in the mid-elevational region determined the distinctive microclimate in MCF.

Besides the visibility measurement during IOP, to demonstrate that the persistent humid conditions events at mid-elevation, we further utilized the RH measurement along the elevation as the proxy for the environment's wetness. As shown in Table 1, the daily and daytime mean of RH in the understory in CCH were significantly wetter at mid-elevation than other elevation on no-rain days. The remarkably humid characteristic at mid-elevation validates the unique feature of MCF and the discontinuous change of DTR in altitude.

Seasonal variations in DTR occurred along the elevation, but the discontinuity in DTR was still evident in every season (Fig. S1). In mountainous regions, the complicated topographic shade and diverse dense canopy might exert a complex influence on the spatial variation in the DTR. Accordingly, we further investigate the seasonality of elevational discontinuity in DTR and RH. From the results in the open field, a slight seasonal influence of fog and low-clouds on DTR in the spring (Fig. S2a). Still, the mid-elevational region's DTR (Fig. S2) is narrower and RH (Table S1) is higher than that in other elevational areas in all seasons. Moreover, no consistent effects of topographic aspect and LAI was observed on the DTR along the observational transect (Fig. S3). Therefore, fog might be a primary reason explaining the discontinuity in the DTR at high altitudes of the CCH.

Furthermore, in MCFs, the T_{\max}^{open} and T_{\max}^{under} were significantly lower than in other elevated regions, which might be remarkably affected by the fog (Fig. 3c, d). However, the T_{\min}^{open} and T_{\min}^{under} in the MCFs were similar with low elevations, and its variations diverged. The T_{\min}^{open} in the MCFs was warmer compared with that in high altitude regions, probably due to the warming effect of the downward longwave radiation by fog. The T_{\max}^{under} in the MCFs was much lower, and even if a nighttime warming effect of fog existed in the MCFs, the T_{\min}^{under} was frequent cooler than that at a high altitude. Thus, a significant discontinuity of the DTR along the altitude was most likely due to a smaller T_{\max} in the MCFs of the CCH.

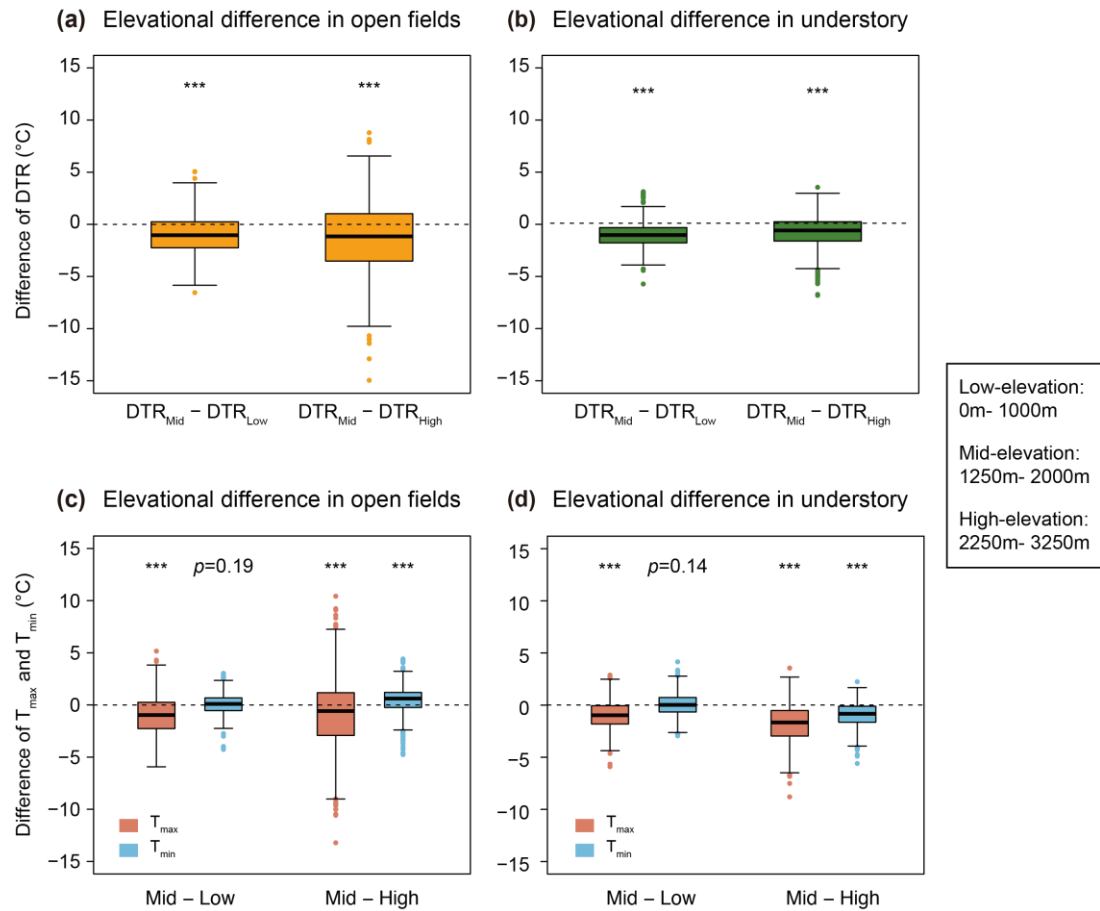


Figure 3. Elevational difference of detrended DTR, T_{\max} , and T_{\min} between mid-elevation and low-elevation (left) and between mid-elevation and high-elevation (right) in (a, c) open fields and (b, d) understory. The box represents the 25th and 75th percentile along with the median of 2018–2019 daily data. The upper and lower fences represent 1.5 times the interquartile range. Solid dots represent potential outliers. The p values were obtained from one-tailed tests, and *** indicates a 0.1% significant difference.

(mean \pm std)

Site	Plot	Daily mean of RH in foggy days	Daily mean of RH in clear days	Daytime mean of RH in foggy days	Daytime mean of RH in clear days
Chi-Lan	Understory	98.8% \pm 3.5%	93.3% \pm 9.6%	98.4% \pm 4.2%	91.5% \pm 10.1%
Site	Elevational region	Daily mean of RH		Daytime mean of RH	
CCH	High	87.2% \pm 12.4%*		85.3% \pm 12.5%*	
	Mid	93.6% \pm 6.8%		91.6% \pm 7.3%	

Low

 $87.3\% \pm 10.6\%^*$ $80.8\% \pm 10.1\%^*$

*Significant difference from mid-elevation at the 1% significance level (one-tailed t test)

Table 1. The daily and daytime (6:00–18:00) average of the RH in the understory at CCH (IOP, 2017/04/25– 06/7) and Chi-Lan (2020/01/15– 04/30) on no-rain days. In Chi-Lan, we separated foggy and clear days utilizing visibility data.

4 Discussion

This study shows that a significant elevational trend of the DTR is apparent over open fields but not in the understory. The variation of the DTR at an altitude between two fields demonstrates a substantial modulation by the canopy for the microclimate at a high altitude (Fig. 2). Solar radiation is usually the dominant factor affecting the T_{\max} , which is competently reduced by canopy cover. Due to the shadowing effect and the heat storage of the crown, the canopy cover effect could smoothen the elevational heterogeneity of the DTR, reducing climatic variability with altitude in the understory. The non-significant elevational trend of DTR in the understory was mentioned, but the effect of canopy shape on the DTR cannot be determined clearly by the comparison in coarse resolution (Rapp & Silman, 2012). Our in situ paired experiments emphasized the contrast elevational trend of DTR within a short distance (< 500 m) between the understory and open field. The impact of canopy shape differed with respect to DTR, particularly at high elevations. As the elevation increased, the DTR significantly increased in the absence of forest cover. This considerable difference underscores the importance of observing the understory microclimate. Furthermore, in mountainous regions, the elevation provides a continuous altitudinal gradient of mean temperature and regulates deforestation-induced warming (Zeng et al., 2021). Even in MCFs, changes in land use could irretrievably affect the functions of the local ecosystem (Hamilton, 1995; Ledo et al., 2009).

In addition to the aforementioned biotic factors, abiotic factors severely influence the microclimate in mountainous regions. From our results, fog and low-clouds create altitudinal discontinuities in DTR and highlights the irreplaceable microclimatological characteristics of MCFs through the high-resolution continuous observation in altitude across non-cloud forest and MCFs. The DTR significantly becomes narrower at MCFs in both the understory and open field. Hence, species at the MCFs necessarily encounter greater climate variability if they shift to a higher altitude for cooler habitats. The discontinuity of the DTR makes mid-elevational habitats particularly crucial because species cannot find such an environment with a small DTR along the elevation. If environmental changes along the elevation are assumed to be linear or if the weather conditions of open fields are used for the forest understory ecosystem, the distribution or behavior of species might be misinterpreted. In addition, most previous studies focused on the temporal variation of DTR or conducted integrated analyses on large spatial scales. Only a few studies have analyzed high-resolution spatial variability of the DTR, in which they have demonstrated that the elevational trends of DTR exhibit unimodal curves or nonlinear patterns along the elevation gradients in open fields (Gheyret et al., 2020; Rapp & Silman, 2012; Wang et al., 2017; Xue et al., 2020). Observations in the CCH at >3000 m a.s.l. also demonstrated the unimodal distribution of the DTR. Yet, the mechanisms behind the diverse trends of DTR in

altitude were not clarified in previous studies. Overall, the continuous observation with high-resolution we conducted in CCH demonstrated the dynamic fog and low-clouds were the primary contributors to the nonlinear changes in the DTR along the elevation in the understory and open fields.

Based on Schulz et al. (2017), our results explicitly infer the frequent foggy events generate the elevational discontinuity in the DTR using continuous in-situ observations along an elevation gradient. Fog efficiently mitigates the increasing temperature during daytime by increasing the albedo. Furthermore, the considerable radiative warming effect by the emitted downward longwave radiation from fog would even be comparable with that from the cloud (Guo et al., 2021). In addition to the topography, vegetation, and precipitation, fog occurrence is a critical factor that alters the elevational variation in the DTR. However, with the increasing temperature caused by global warming and urbanization, the altitude and frequency of fog occurrence and cloud base might be altered due to the lack of water vapor condensation (Foster, 2001; Still et al., 1999). Thus, variation in fog and cloud dynamics under climate change might complicate predictions of how changes in DTR and DTR pose a threat to species in mountainous regions. Therefore, we should further explore how the fog affects microclimate and species in the MCF under climate change.

5 Conclusions

Biotic and abiotic factors jointly influence the spatial heterogeneity of the microclimate. The tree canopy's shade effectively prevents the heating effect by solar radiation, decreasing the T_{\max}^{under} and T_{\min}^{under} . The DTR significantly increases at higher altitudes in open sites. Nevertheless, no significant elevational trends of DTR were observed in the understory. Due to differing elevational trends of the DTR, canopy mitigation is broader at high elevations; therefore, the forests are vital for the species living in stable and comfortable habitats at high elevations. Furthermore, the elevational trends of the DTR are discontinuous both in the understory and open fields. The discontinuity of elevational trend in DTR caused by the narrower DTR in the MCFs. The reduction of downward solar radiation by fog significantly reduces the T_{\max} in the mid-elevation than at other elevational regions at both sites. Besides, fog traps the longwave radiation to reduce the cooling rate in the mid-elevation and keep the T_{\min} at a warmer level relative to those at other elevational ranges. The discontinuity of DTR makes mid-elevation home to irreplaceable and valuable habitats. This study highlights the essential and considerable effect of fog and canopy on climatic variability, particularly in the mid- and high-elevational regions. Because of unique characteristics of the microclimate in MCFs, the complex hydro-climatological cycle in montane regions must be urgently evaluated.

Acknowledgments

We sincerely acknowledge Mr. Wei-Ping Chan, Mr. Tzu-Neng Yuan, Ms. Hsiang-Yu Tsai, Ms. Ting-Chu Hsieh, as well as Ms. Rong-Yu Gu for the assistant in field work and discussion. This study was supported by the NTU Core Consortiums Project (NTUCC-109L892805) and the Ministry of Science and Technology grants of 106-2111-M-002-010-MY4 and 110-2628-M-002-004-MY4 to National Taiwan University. This article was subsidized for English editing by National Taiwan University under the Excellence Improvement Program for Doctoral Students (grant number 108-2926-I-002-002-MY4), sponsored by Ministry of Science and Technology, Taiwan. S.-F.S. was supported by Academia Sinica (AS-SS-106-05, AS-SS-110-05 and , NTU-

AS-107L104316) and Minister of Science and Technology, Taiwan (MOST 108-2314-B-001-009-MY3).

Open research

The near-surface air temperature in the open field of Yuanyanghu weather station (C0UA1) is able to be downloaded from the Data Bank for Atmospheric and Hydrologic Research (<https://dbar.pccu.edu.tw/>) after registration (Only available in Traditional Chinese). The elevation data from 30-meter Advanced Spaceborne Thermal Emission and Reflection Radiometer Global Digital Elevation Model version 2.0 are download from Center for GIS, Research Center for humanities and Social Sciences, Academia Sinica data server (<http://gis.rchss.sinica.edu.tw/qgis/?p=1619>). All results were analyzed and visualized by using R version 3.6.3. The data and the codes for analyses are compiled on the Zenodo data repository (<https://doi.org/10.5281/zenodo.5864982>).

References

- Beers, T. W., Dress, P. E., & Wensel, L. C. (1966). Notes and observations: aspect transformation in site productivity research. *Journal of Forestry*, 64(10), 691–692.
- Braganza, K., Karoly, D. J., & Arblaster, J. M. (2004). Diurnal temperature range as an index of global climate change during the twentieth century. *Geophysical Research Letters*, 31(13), 2–5. <https://doi.org/10.1029/2004GL019998>
- Bruijnzeel, L. A., Scatena, F. N., & Hamilton, L. S. (2011). *Tropical montane cloud forests: science for conservation and management*. Cambridge University Press.
- Chan, S., Shih, W., Chang, A., Shen, S., & Chen, I. (2019). Contrasting forms of competition set elevational range limits of species. *Ecology Letters*, 22(10), 1668–1679.
- Chan, W.-P., Chen, I.-C., Colwell, R. K., Liu, W.-C., Huang, C. -y., & Shen, S.-F. (2016). Seasonal and daily climate variation have opposite effects on species elevational range size. *Science*, 351(6280), 1437–1439. <https://doi.org/10.1126/science.aab4119>
- Chen, I.-C., Shiu, H.-J., Benedick, S., Holloway, J. D., Chey, V. K., Barlow, H. S., et al. (2009). Elevation increases in moth assemblages over 42 years on a tropical mountain. *Proceedings of the National Academy of Sciences*, 106(5), 1479–1483.
- Chu, H. Sen, Chang, S. C., Klemm, O., Lai, C. W., Lin, Y. Z., Wu, C. C., et al. (2014). Does canopy wetness matter? Evapotranspiration from a subtropical montane cloud forest in Taiwan. *Hydrological Processes*, 28(3), 1190–1214. <https://doi.org/10.1002/hyp.9662>
- Dai, A., Trenberth, K. E., & Karl, T. R. (1999). Effects of clouds, soil moisture, precipitation, and water vapor on diurnal temperature range. *Journal of Climate*, 12(8 PART 2), 2451–2473. [https://doi.org/10.1175/1520-0442\(1999\)012<2451:eocsmp>2.0.co;2](https://doi.org/10.1175/1520-0442(1999)012<2451:eocsmp>2.0.co;2)
- Easterling, D. R., Horton, B., Jones, P. D., Peterson, T. C., Karl, T. R., Parker, D. E., et al. (1997). Maximum and minimum temperature trends for the globe. *Science*, 277(5324), 364–367. <https://doi.org/10.1126/science.277.5324.364>
- Foster, P. (2001). The potential impacts of global climate change on tropical montane cloud forests. *Earth-Science Reviews*, 55(1–2), 73–106. [https://doi.org/10.1016/S0012-8252\(01\)00056-3](https://doi.org/10.1016/S0012-8252(01)00056-3)
- De Frenne, P., Rodríguez-Sánchez, F., Coomes, D. A., Baeten, L., Verstraeten, G., Vellen, M., et al. (2013). Microclimate moderates plant responses to macroclimate warming. *Proceedings of the National Academy of Sciences of the United States of America*, 110(46), 18561–18565. <https://doi.org/10.1073/pnas.1311190110>

- Gheyret, G., Mohammat, A., & Tang, Z. (2020). Elevational patterns of temperature and humidity in the middle Tianshan Mountain area in Central Asia. *Journal of Mountain Science*, 17(2), 397–409.
- Gu, R.-Y., Lo, M.-H., Liao, C.-Y., Jang, Y.-S., Juang, J.-Y., Huang, C.-Y., et al. (2021). Early Peak of Latent Heat Fluxes Regulates Diurnal Temperature Range in Montane Cloud Forests. *Journal of Hydrometeorology*.
- Guo, L., Guo, X., Luan, T., Zhu, S., & Lyu, K. (2021). Radiative effects of clouds and fog on long-lasting heavy fog events in northern China. *Atmospheric Research*, 252, 105444.
- Hamilton, L. S. (1995). Mountain cloud forest conservation and research: a synopsis. *Mountain Research and Development*, 259–266.
- Hansen, J., Sato, M., & Ruedy, R. (1995). Long-term changes of the diurnal temperature cycle: Implications about mechanisms of global climate change. *Atmospheric Research*, 37(1–3), 175–209.
- Hijmans, R. J., Van Etten, J., Cheng, J., Mattiuzzi, M., Sumner, M., Greenberg, J. A., et al. (2015). Package ‘raster.’ *R Package*, 734.
- Hufkens, K., Basler, D., Milliman, T., Melaas, E. K., & Richardson, A. D. (2018). An integrated phenology modelling framework in R. *Methods in Ecology and Evolution*, 9(5), 1276–1285.
- Jaagus, J., Briede, A., Rimkus, E., & Remm, K. (2014). Variability and trends in daily minimum and maximum temperatures and in the diurnal temperature range in Lithuania, Latvia and Estonia in 1951–2010. *Theoretical and Applied Climatology*, 118(1–2), 57–68. <https://doi.org/10.1007/s00704-013-1041-7>
- Jackson, L. S., & Forster, P. M. (2010). An empirical study of geographic and seasonal variations in diurnal temperature range. *Journal of Climate*, 23(12), 3205–3221. <https://doi.org/10.1175/2010JCLI3215.1>
- Karl, T. R., Knight, R. W., Gallo, K. P., Peterson, T. C., Jones, P. D., Kukla, G., et al. (1993). A New Perspective on Recent Global Warming: Asymmetric Trends of Daily Maximum and Minimum Temperature. *Bulletin of the American Meteorological Society*. [https://doi.org/10.1175/1520-0477\(1993\)074<1007:ANPORG>2.0.CO;2](https://doi.org/10.1175/1520-0477(1993)074<1007:ANPORG>2.0.CO;2)
- Kassambara, A. (2020). rstatix: pipe-friendly framework for basic statistical tests. R package version 0.4.0. Available Online at: <https://Cran.r-Project.Org/Web/Packages/Rstatix/Index>.
- Kerr, J. T., Pindar, A., Galpern, P., Packer, L., Potts, S. G., Roberts, S. M., et al. (2015). Climate change impacts on bumblebees converge across continents. *Science*, 349(6244), 177–180.
- Klinges, D. H., & Scheffers, B. R. (2021). Microgeography, not just latitude, drives climate overlap on mountains from tropical to polar ecosystems. *American Naturalist*, 197(1), 75–92. <https://doi.org/10.1086/711873>
- Körner, C. (2004). Mountain biodiversity, its causes and function. *AMBIO: A Journal of the Human Environment*, 33(sp13), 11–17.
- Kumar, K. R., Kumar, K. K., & Pant, G. B. (1994). Diurnal asymmetry of surface temperature trends over India. *Geophysical Research Letters*, 21(8), 677–680. <https://doi.org/10.1029/94GL00007>
- Ledo, A., Montes, F., & Condes, S. (2009). Species dynamics in a montane cloud forest: Identifying factors involved in changes in tree diversity and functional characteristics. *Forest Ecology and Management*, 258, S75–S84.
- Myers, N., Mittermeier, R. A., Mittermeier, C. G., Da Fonseca, G. A. B., & Kent, J. (2000). Biodiversity hotspots for conservation priorities. *Nature*, 403(6772), 853–858.

- Pepin, Nick, Deng, H., Zhang, H., Zhang, F., Kang, S., & Yao, T. (2019). An Examination of Temperature Trends at High Elevations Across the Tibetan Plateau: The Use of MODIS LST to Understand Patterns of Elevation-Dependent Warming. *Journal of Geophysical Research: Atmospheres*, 124(11), 5738–5756. <https://doi.org/10.1029/2018JD029798>
- Pepin, Nicolas, Bradley, R. S., Diaz, H. F., Baraër, M., Caceres, E. B., Forsythe, N., et al. (2015). Elevation-dependent warming in mountain regions of the world. *Nature Climate Change*, 5(5), 424–430.
- Rapp, J. M., & Silman, M. R. (2012). Diurnal, seasonal, and altitudinal trends in microclimate across a tropical montane cloud forest. *Climate Research*, 55(1), 17–32. <https://doi.org/10.3354/cr01127>
- Rumpf, S. B., Hülber, K., Klonner, G., Moser, D., Schütz, M., Wessely, J., et al. (2018). Range dynamics of mountain plants decrease with elevation. *Proceedings of the National Academy of Sciences*, 115(8), 1848–1853.
- Scheffers, B. R., Edwards, D. P., Diesmos, A., Williams, S. E., & Evans, T. A. (2014). Microhabitats reduce animal's exposure to climate extremes. *Global Change Biology*, 20(2), 495–503. <https://doi.org/10.1111/gcb.12439>
- Schulz, H. M., Li, C.-F., Thies, B., Chang, S.-C., & Bendix, J. (2017). Mapping the montane cloud forest of Taiwan using 12 year MODIS-derived ground fog frequency data. *PloS One*, 12(2).
- Shekhar, M. S., Devi, U., Dash, S. K., Singh, G. P., & Singh, A. (2018). Variability of Diurnal Temperature Range During Winter Over Western Himalaya: Range- and Altitude-Wise Study. *Pure and Applied Geophysics*, 175(8), 3097–3109. <https://doi.org/10.1007/s00024-018-1845-6>
- Shen, X., Liu, B., Li, G., Wu, Z., Jin, Y., Yu, P., & Zhou, D. (2014). Spatiotemporal change of diurnal temperature range and its relationship with sunshine duration and precipitation in China. *Journal of Geophysical Research: Atmospheres*, 119(23), 13–163.
- Still, C. J., Foster, P. N., & Schneider, S. H. (1999). Simulating the effects of climate change on tropical montane cloud forests. *Nature*, 398(6728), 608–610.
- Tsai, H.-Y., Rubenstein, D. R., Fan, Y.-M., Yuan, T.-N., Chen, B.-F., Tang, Y., et al. (2020). Locally-adapted reproductive photoperiodism determines population vulnerability to climate change in burying beetles. *Nature Communications*, 11(1), 1–12.
- Vose, R. S., Easterling, D. R., & Gleason, B. (2005). Maximum and minimum temperature trends for the globe: An update through 2004. *Geophysical Research Letters*, 32(23), 1–5. <https://doi.org/10.1029/2005GL024379>
- Wang, G. yi, Zhao, M. fei, Kang, M. yi, Xing, K. xiong, Wang, Y. hang, Xue, F., & Chen, C. (2017). Diurnal and seasonal variation of the elevation gradient of air temperature in the northern flank of the western Qinling Mountain range, China. *Journal of Mountain Science*, 14(1), 94–105. <https://doi.org/10.1007/s11629-016-4107-z>
- Xue, F., Jiang, Y., Wang, M., Dong, M., Ding, X., Yang, X., & Kang, M. (2020). Temperature and thermal growing season variations along elevational gradients on a sub-alpine, temperate China. *Theoretical and Applied Climatology*, 140(1), 15–24.
- Zellweger, F., Coomes, D., Lenoir, J., Depauw, L., Maes, S. L., Wulf, M., et al. (2019). Seasonal drivers of understorey temperature buffering in temperate deciduous forests across Europe. *Global Ecology and Biogeography*, 28(12), 1774–1786. <https://doi.org/10.1111/geb.12991>
- Zeng, Z., Wang, D., Yang, L., Wu, J., Ziegler, A. D., Liu, M., et al. (2021). mountain regions regulated by elevation. *Nature Geoscience*, 14(January). <https://doi.org/10.1038/s41561->

020-00666-0

Zhang, Y., Shen, X., & Fan, G. (2021). Elevation-dependent trend in diurnal temperature range
in the northeast china during 1961–2015. *Atmosphere*, 12(3), 1–11.
<https://doi.org/10.3390/atmos12030319>